

Theoretical fits of the δ Cephei light, radius and radial velocity curves

Giovanni Natale^{1,2}, Marcella Marconi², Giuseppe Bono³

ABSTRACT

We present a theoretical investigation of the light, radius and radial velocity variations of the prototype δ Cephei. We find that the best fit model accounts for luminosity and velocity amplitudes with an accuracy better than 0.8σ , and for the radius amplitude with an accuracy of 1.7σ . The chemical composition of this model suggests a decrease in both helium (0.26 vs 0.28) and metal (0.01 vs 0.02) content in the solar neighborhood. Moreover, distance determinations based on the fit of light curves agree at the 0.8σ level with the trigonometric parallax measured by the Hubble Space Telescope (HST). On the other hand, distance determinations based on angular diameter variations, that are independent of interstellar extinction and of the p -factor value, indicate an increase of the order of 5% in the HST parallax.

Subject headings: Cepheids – stars: distances – stars: evolution – stars: oscillations

1. Introduction

Classical Cepheids are the most important primary distance indicators. One of the key issues concerning the use of Cepheids as distance indicators is their dependence on chemical composition. Empirical tests seem to suggest that metal-rich Cepheids are, at fixed period, brighter than metal-poor ones, either over the entire period range (Kennicutt et al. 1998, 2003; Kanbur et al. 2003; Storm et al. 2004; Groenewegen et al. 2004; Sakai et al. 2004;

¹Max-Planck-Institut fuer Kernphysik Saupfercheckweg 1, D-69117 Heidelberg (current position), giovanni.natale@mpi-hd.mpg.de

²INAF-Osservatorio Astronomico di Capodimonte, Via Moiariello 16, 80131 Napoli, Italy; marcella@oacn.inaf.it

³INAF-Osservatorio Astronomico di Roma, Via Frascati 33, 00040 Monte Porzio Catone, Italy; bono@mporzio.astro.it

Macri et al. 2006) or for periods shorter than ≈ 25 days (Sasselov et al. 1997; Sandage et al. 2004). On the other hand, distance estimates based on the Near-Infrared Surface Brightness method indicate that the slope of the Period-Luminosity (PL) relation might be the same for Magellanic and Galactic Cepheids (Gieren et al. 2005). However, the impact of the projection factor p on the Cepheid distances is still debated (Saha et al. 2006; Nardetto et al. 2007). Early theoretical predictions based on linear pulsation models (e.g. Sandage et al. 1999; Alibert et al. 1999; Baraffe & Alibert 2001) predicted a mild metallicity effect, while nonlinear convective models (Bono et al. 1999; Caputo et al. 2002; Fiorentino et al. 2002; Marconi et al. 2005) showed that the metallicity affects both the zero-point and the slope of the PL relations. This effect is more evident in the optical bands and it is nonlinear when moving from metal-poor ($Z = 0.004$) to super metal-rich ($Z = 0.04$) structures. Current predictions also suggest a turnover across solar metallicity ($Z \sim 0.02$) due to the correlated increase in He content (Fiorentino et al. 2002; Marconi et al. 2005).

Three approaches are adopted to calibrate the Cepheid PL relations: cluster distances, trigonometric parallaxes and Baade-Wesselink (BW) method. Parallaxes based on Cepheids in open clusters and associations have been widely adopted to calibrate the PL relations (Turner & Burke 2002), but Fouque et al. (2007) found a systematic difference with other methods. Accurate Cepheid parallaxes have been provided by Benedict et al. (2002) and by Benedict et al. (2007) using the Fine Guide Sensor on board the Hubble Space Telescope (HST). They measured the distance of several Galactic Cepheids with average relative errors of $\approx 8\%$. The BW method appears to be a robust approach, but some assumptions need to be investigated (Gautschy 1987; Bono et al. 1994; Gieren et al. 2005). The value of the projection factor (p), i.e. the parameter adopted to transform radial into pulsation velocity, is still controversial (Sabbey et al. 1995; Mérand et al. 2006). The typical value used in the literature is $p = 1.36$ (Burki et al. 1982), but period-dependent values are also adopted (Gieren et al. 1993, 2005). However, the p -factor of δ Cephei, $p = 1.27 \pm 0.06$, measured by Mérand et al. (2005), using the HST parallax, agrees quite well with the predicted value (Nardetto et al. 2004).

Although, several Cepheids are binaries dynamical mass estimates are only available for a handful objects (Evans et al. 2005). Current mass estimates rely either on evolutionary or on pulsation prescriptions (D’Cruz et al. 2000; Keller & Wood 2002; Caputo et al. 2005) and we are still facing the long-standing problem of the “Cepheid mass discrepancy” (Cox 1980). Evolutionary masses are systematically larger than pulsation masses (Bono et al. 2001; Beaulieu et al. 2001; Caputo et al. 2005).

Theoretical fits of Cepheid light curves provide robust constraints on their intrinsic parameters and distances (Wood et al. 1997; Bono et al. 2002; Keller & Wood 2006). This

approach, up to now, has only been applied to Bump Cepheids. We present, for the first time, a simultaneous fit of optical/NIR light, radial velocity, and angular diameter variations of the prototype δ Cephei. We selected this object because accurate measurements of light, radius, velocity curves, and of the p -factor are available and its geometric distance is known with an accuracy of 4% (273_{-11}^{+12} Benedict et al. 2002).

2. Empirical and theoretical framework

The optical (V, I) and the near-infrared (NIR) K -band light curve were collected by Kiss (1998) and by Barnes et al. (1997). We selected these light curves because both the shape and the amplitude in the optical bands depend on surface temperature and radius variation, while in K -band the dependence on temperature is significantly reduced. The radial velocity data were collected by Bersier et al. (1994)¹, while the angular diameter and the projection factor by Mérand et al. (2005). The observables for δ Cephei are summarized in Table 1.

The adopted theoretical framework is based on a nonlinear radial pulsation code, including the nonlocal and time-dependent treatment of turbulent convection ((Stellingwerf 1982; Bono & Stellingwerf 1994; Bono et al. 1999). The system of nonlinear equations is closed using a free parameter, α_{ml} , that is proportional to the mixing length parameter. Changes in the α_{ml} parameter affect, as expected, both the limit cycle stability (pulsation amplitudes) and the topology of the instability strip (Fiorentino et al. 2007; Di Criscienzo et al. 2004). Similar approaches for the treatment of convective transport have been developed by Feuchtinger (1999); Buchler & Szabó (2007), and Oliver & Wood (2005).

In order to provide a detailed fit of δ Cephei pulsation properties we adopted three different metal abundances, ranging from $Z = 0.01$ to $Z = 0.02$, to account for current spectroscopic measurements (Fry & Carney 1997) that indicate a metal abundance close to solar ($[Fe/H] = -0.01 \pm 0.06$). Recent spectroscopic measurements of solar heavy element abundances show a significant decrease when compared with previous estimates, and indeed the ratio between heavy-elements and hydrogen, Z/X , decreased from 0.023 (Grevesse & Sauval 1998) to 0.0177 (Lodders 2003) or to 0.0171 (Asplund et al. 2004, 2005). This implies that the surface heavy element abundance of the Sun decreased from $Z = 0.017$ to $Z = 0.0126/0.0133$. The surface He abundance of the Sun according to helioseismological estimates, combined with these latest solar metallicity estimates, is $Y = 0.2485 \pm 0.0034$ (Basu & Antia 2004). However, the new solar photospheric abundances are at odds with helioseismology measurements (Bahcall et al. 2005; Guzik et al. 2005) and, at present, solar models are constructed

¹See the database <http://crocus.physics.mcmaster.ca/Cepheid/>

by adopting protosolar helium abundances ranging from $Y_0 \sim 0.26$ to $Y_0 \sim 0.28$ and heavy metal abundances ranging from $Z_0 = 0.015$ to $Z_0 = 0.02$. According to these evidence we adopted $Z = 0.02$ and $Y = 0.28$ (see Table 2). Once the chemical composition was fixed, we constructed a sequence of isoperiodic pulsation models, by adopting the pulsation relation (the relation connecting the period to stellar mass, luminosity, and effective temperature) provided by Bono et al. (2000). We selected the fundamental models with periods within 2% of the observed period ($P=5.3663$ days, Fernie 1995²) and pulsationally unstable according to the analytical relations for the instability strip boundaries provided by Bono et al. (2000). For each mass value, we fixed the lower limit to the input luminosity according to the Mass-Luminosity (ML) relation given by Bono et al. (2000) and the upper limit according to mild overshooting predictions, i.e. by adding to the quoted value a fixed luminosity excess i.e. $\Delta \log L = 0.25$ (Chiosi et al. 1993). The bolometric light curves were transformed into the UBVIJK photometric bands by adopting the model atmospheres provided by Castelli et al. (1997).

3. Results and discussion

We constructed a sequence of models at fixed chemical composition ($Z = 0.02$, $Y = 0.28$) and by assuming steps in mass and in effective temperature of $\Delta M = 0.5M_\odot$ and $\Delta T_e = 100K$. The comparison between theory and observations indicate that a model with $M = 5.5M_\odot$, and $Te = 5700K$ accounts for the shape of the light curves and for the secondary bump located on the decreasing branch of the radial velocity curve ($\phi \approx 0.2$). To further improve the agreement between predicted and empirical observables, we constructed a new sequence of models by adopting smaller steps in mass and in effective temperature, namely $\Delta M = 0.1M_\odot, \Delta T_e = 25K$. For every model in this sequence, the mixing length parameter was changed from $\alpha_{ml} = 0.3$ to $\alpha_{ml} = 0.4$. Note that an increase in α_{ml} causes a decrease in the pulsation driving, and in turn a decrease in the limit cycle amplitudes. Data plotted in the left panels of Fig. 1 show that the best fit model ($\alpha_{ml} = 0.33$) accounts for the optical and NIR light curves, but both the radial velocity ($\sigma(\Delta V_r) = 4.2$) and the radius ($\sigma(\Delta R) = 3.3$) amplitudes are systematically smaller than the observed ones. This discrepancy can only be removed by decreasing the p -factor from 1.27 to the barely plausible value of $p \sim 1$. To further constrain the impact of the adopted chemical composition on the limit cycle stability, we constructed a new sequence of models by using the same metal abundance and a lower He content ($Y = 0.26$). The new best fit model (see Table 2 and the middle panels of Fig. 1) accounts for optical and NIR light curves and better reproduces

²<http://www.astro.utoronto.ca/DDO/research/cepheids/>

radial velocity ($\sigma(\Delta V_r) = 1.6$) and radius ($\sigma(\Delta R) = 2.3$) variations. The predicted V -band light curve presents a mild discrepancy along the rising branch. However, the discrepancy on luminosity amplitudes is smaller than 0.4σ . In order to verify the occurrence of a degeneracy in the input parameters, we also computed a new series of models by using a lower He content, ($Y = 0.24$, see Table 2 and right panels of Fig. 1). Interestingly enough, velocity and radius amplitudes predicted by new best fit-model are at least 2.5σ smaller than observed. Once again, a reasonable fit between theory and observations would require a barely plausible p -factor ($p = 1.03$).

In order to test how the fits depend on metallicity, we computed a new series of models by adopting $Z = 0.015$, and He content of $Y = 0.27$ (see Table 2). Data plotted in the left panels of Fig. 2 show that the new best fit model agrees reasonably well with the observations. However, the discrepancy in the radial velocity is 1.6σ and in the radius amplitude is 2.5σ . This finding indicates that a decrease in the metal content improves the agreement between theory and observations. Therefore, we constructed two new sequences of pulsation models by adopting a more metal-poor chemical composition ($Z = 0.01$) and two different He contents ($Y = 0.26, 0.24$). The new best fit models (see Table 2, middle and right panels of Fig. 2) account quite well for luminosity, radial velocity, and radius variations. A marginal difference between theory and observations is still present. However, the discrepancy is on average smaller than 1σ for $Y = 0.26$ and systematically larger for $Y = 0.24$ (see Table 2). The comparison between theory and observations brings forward several findings. *i)* the more metal-poor ($Z = 0.01$) best fit models account for the observed light and velocity amplitudes at a level better than 0.8σ and the average discrepancy over the entire cycle is $< 0.2\Sigma$ (see Table 2). *ii)* The fit of the radial velocity curve is very sensitive to the input parameters. The small “bump“ located along the decreasing branch ($\phi = 0.2$) mainly depends on the mass value, and it is independent of the chemical composition. Moreover, the radial velocity amplitude strongly depends on the He content. For example, an increase/decrease of $\sim 8\%$ in He content causes, at $Z=0.02$, an increase on the amplitude discrepancy of at least 1.4σ . The more metal-rich best fit models ($Y=0.28, 0.25$) to properly fit the velocity amplitude would require p -factor values that are at least $\sim 20\%$ smaller than the empirical measurement by Mérand et al. (2006). Therefore, they do not pass the empirical validation. *iii)* Predicted radius variations are at least 1.7σ smaller than observed while the average discrepancy over the entire curve is never smaller than 0.2Σ for all the adopted chemical compositions. The mismatch is mainly caused by the few points located across the phases of minimum radius. We do not have a firm explanation for this discrepancy. These phases are the most rapid ones along the pulsation cycle and the radial displacements of the outermost layers might be affected either by shock waves or by velocity gradients (Mathias et al. 2006). This critical point deserves further investigations, since radius measurements depend on the adopted

distance and on limb darkening correction, but they are affected neither by the interstellar extinction nor by the p -factor. Therefore, they can play a key role in constraining theoretical predictions. *iv*) The model with $Z = 0.01$ and $Y = 0.26$ provides the optimum fit to all observables (except for the only three magnitudes on the rising branch of the V light curve). This finding taken at face value indicates that the He content might be 8% smaller than typically assumed to construct Galactic Cepheid models. The metal content of δ Cephei seems to be 0.1–0.2 dex more metal-poor than suggested by spectroscopy, but this constraint is less robust. Note that the p -factor adopted for this model ($p = 1.28$) agrees quite well with the measurement by Mérand et al. (2006). *v*) The best fit models present a luminosity excess (see column 7 in Table 2) that ranges from $\Delta \text{Log}L/L_{\odot} = 0.07$ ($Z=0.01$, $Y=0.26$) to 0.17 ($Z=0.02$, $Y=0.24$). These values are between the luminosities predicted by a canonical ML relation (Bono et al. 2000) and those predicted by mild core overshooting ML relation ($\Delta \text{Log}L = 0.25$, Chiosi et al. 1993).

As a further validation of the current approach, we also estimated the absolute distance to δ Cephei using the best fit models that passed the empirical validations. In order to provide a plausible estimate of the errors affecting distance determinations we assumed the largest uncertainties on the adopted input parameters: $\Delta M = 0.1M_{\odot}$, $\Delta T = 50K$, $\Delta \text{Log}L = 0.02$, $\Delta R = 0.5R_{\odot}$. By accounting for the entire error budget the intrinsic uncertainties on current distance determinations is about 3% for photometric distances and ≈ 5 pc for the distances derived from the fit of radius variations. Distance estimates based on the apparent distance moduli provided by the fit of both optical and NIR light curves and on the reddening law provided by Cardelli et al. (1989) are listed in columns 6 and 7 of Table 3. The comparison with the HST parallax shows that distances based on V, I -bands agree at the 0.2σ level, while those based on the V, K -bands are within 0.8σ level. Errors either in the photometric zero-points or in the adopted color-temperature transformations or in the extinction law account for the difference in the distance determinations based on light curves. Moreover, the occurrence of a circumstellar envelope (CSE) around δ Cephei (Mérand et al. 2006) could also affect the reddening corrections due to the different relative distribution of the absorbing grains around the star, compared to typical interstellar medium distribution. Independent distance determinations follow from comparing the observed angular diameter variations by Mérand et al. (2005) with the radius curves from four different models. The distances (Table 3, column 8) agree well with each other and are on average only 5% (1.3σ) larger than the trigonometric distance. The comparison of observed and model radii is in principle a powerful method to derive Cepheid distances, since it is independent of the assumption on the p -factor and on interstellar extinction. Note that an increase in the distance would also imply an increase in the p -factor, since at fixed radial velocity amplitude, $p \propto \Delta\Theta \cdot d$, where $\Delta\Theta$ is the angular diameter amplitude.

Finally we mention that the mean radii predicted by the best fit models match within 1σ the empirical estimate based on the angular diameter provided by ME06 ($R = 43 \pm 2R_{\odot}$), by assuming the HST parallax.

It is a pleasure to thank A. Mérand for several interesting discussions on interferometric measurements. We also acknowledge an anonymous referee for a detailed and helpful report.

REFERENCES

- Alibert, Y., Baraffe, I., Hauschildt, P., Allard, F. 1999, *A&A*, 344, 551
- Asplund, M., Grevesse, N., Sauval, A. J., Allende Prieto, C., Kiselman, D. 2004, *A&A*, 417, 751
- Asplund, M., Grevesse, N., Sauval, A. J., Allende Prieto, C., Blomme, R. 2005, *A&A*, 431, 693
- Bahcall, J. N., Basu, S., Pinsonneault, M., Serenelli, A. M. 2005, *ApJ*, 618, 1049
- Baraffe, I., Alibert, Y. 2001, *A&A*, 371, 592
- Basu, S., Antia, H.M. 2004, *ApJ*, 606, 85
- Barnes, T. G., Fernley, J. A., Frueh, M.L., Navas, J.G., Moffett, T.J., Skillen, I. 1997, *PASP*, 109, 645
- Beaulieu, J. P., Buchler, J. R., Kollth, Z. 2001, *A&A*, 373, 164
- Benedict, G. F., McArthur, B. E., Fredrick, L. W. et al., 2002, *AJ*, 124, 1695
- Benedict, G. F., McArthur, B. E., Feast M. W. et al., 2007, *AJ*, 133, 1810
- Bersier, D., Burki, G., Mayor, M., Duquennoy, A. 1994, *A&AS*, 108, 25
- Bono, G., Caputo, F., Cassisi, S., Marconi, M., Piersanti, L., Tornambé 2000a, *ApJ*, 529, 293
- Bono, G., Gieren, W. P., Marconi, M., Fouqu, P., Caputo, F. 2001, *ApJ*, 563, 319
- Bono, G., Caputo, F., Stellingwerf, R. F. 1994, *ApJ*, 432, L51
- Bono, G., Castellani, V., Marconi, M. 2000b, *ApJ*, 529, 293

- Bono, G., Castellani, V., Marconi, M. 2002, ApJ, 565, L83
- Bono, G., Marconi, M. Stellingwerf, R.F. 1999, ApJS, 122, 167
- Bono, G., Stellingwerf, R.F. 1994, ApJS, 93, 233
- Buchler, J. R., Szabó, R. 2007, ApJ, 660, 723
- Burki, G., Mayor, M., Benz W. 1982, A&A, 109, 258
- Caputo, F., Bono, G., Fiorentino, G., Marconi, M., Musella, I. 2005, ApJ, 629, 1021
- Caputo, F., Marconi, M., Musella, I. 2002, ApJ, 566, 833
- Cardelli, J.A., Clayton, G.C., Mathis, J.S. 1989, ApJ, 345, 245
- Casagrande, L., Flynn, C., Portinari, L., Girardi, L., Jimenez, R. 2007, MNRAS, in press
(astro-ph/0703766)
- Castelli, F., Gratton, R. G., & Kurucz, R. L. 1997, A&A, 324, 432
- Chiosi, C., Wood, P. R., Capitanio, J.S. 1993, ApJS, 86, 541
- Cox, A. N. 1980, ARA&A, 18, 15
- D’Cruz, N. L., Morgan, S. M., Bhm-Vitense, E. 2000, AJ, 120, 990
- Di Criscienzo, M., Marconi, M., Caputo, F. 2004, ApJ, 612, 1092
- Evans, N. R., Carpenter, K. G., Robinson, R., Kienzle, F., Dekas, A. E. 2005, AJ, 130, 789
- Feuchtinger, M. U., 1999, A&AS, 136, 217
- Fiorentino, G., Caputo, F., Marconi, M., Musella, I. 2002, ApJ, 576, 402
- Fiorentino, G., Marconi, M., Musella, I., F. Caputo 2007, A&A, in press
- Fouque, P. et al. 2007, A&A, in press (arXiv:0709.3255)
- Fry, A. M., Carney, B. W. 1997, AJ, 113, 1073
- Gautschy, A., 1987, Vistas in Astronomy, 30, 197
- Gieren, W.P., Barnes, T.G.III, Moffett, T.J. 1993, ApJ, 418, 135
- Gieren, W. P., Storm, J., Barnes, T.G.III, Fouqu’e, P., Pietrznyn’ski, G., Kienzle, F. 2005, ApJ, 627, 224

- Grevesse, N., Sauval, A. J. 1998, *Space Science Reviews*, 85, 161
- Groenewegen, M. A. T., Romaniello, M., Primas, F., Mottini, M. 2004, *A&A*, 420, 655
- Guzik, J. A., Watson, L. Scott, Cox, A. N. 2005, *ApJ*, 627, 1049
- Kanbur, S. M., Ngeow, C., Nikolaev, S., Tanvir, N. R., Hendry, M. A. 2003, *A&A*, 411, 361
- Keller, S.C., Wood, P.R. 2002, *ApJ*, 578, 144
- Keller, S.C., Wood, P.R. 2006, *ApJ*, 642, 834
- Kennicutt, R. C. Jr, et al. 1998, *ApJ*, 498, 181
- Kennicutt, R. C. Jr., et al., 2003, *ApJ*, 591, 801
- Kiss, L. L. 1998, *MNRAS*, 297, 825
- Lodders, K. 2003, *ApJ*, 591, 1220
- Macri, L. M., Stanek, K. Z., Bersier, D., Greenhill, L. J., Reid, M. J. 2006, *ApJ*, 652, 1133
- Marconi, M., Clementini, G. 2005, *AJ*, 129, 2257
- Marconi, M., Musella, I. Fiorentino, G. 2005, *ApJ*, 632, 590
- Mathias, P., Gillet, D., Fokin, A. B., Nardetto, N., Kervella, P., Mourard, D. 2006, *A&A*, 457, 575
- Mérand, A., et al. 2005, *A&A*, 438, 9
- Mérand, A., et al. 2006, *A&A*, 453, 155
- Nardetto, N., Fokin, A., Mourard, D., Mathias, Ph., Kervella, P., Bersier, D. 2004, *A&A*, 428, 131
- Nardetto, N., Mourard, D., Mathias, Ph., Fokin, A., Gillet, D. 2007, *A&A*, 471, 661
- Olivier, E. A., Wood, P. R. 2005, *MNRAS*, 362, 1396
- Sabbey, C. N., Sasselov, D. D., Fieldus, M. S., Lester, J. B., Venn, K. A., Butler, R. P. 1995, *ApJ*, 446, 250
- Saha, A., Thim, F., Tammann, G.A., Reindl, B., Sandage, A. 2006, *ApJS*, 165, 108
- Sakai, S., Ferrarese, L., Kennicutt, R. C., Jr., Saha, A. 2004, *ApJ*, 608, 42

Sandage, A., Bell, R. A., Tripicco, M. J. 1999, ApJ, 522, 250

Sandage, A., Tammann, G. A., Reindl, B.A. 2004, A&A, 424, 43

Sasselov, D. D., et al., 1997, A&A, 324, 471

Stellingwerf 1982, ApJ, 262, 330

Storm, J., Carney, B. W., Gieren, W. P. et al., 2004, A&A, 415, 531

Turner, D. G., Burke, J. F. 2002, AJ, 124, 2931

Wood, P. R., Arnold, A., Sebo, K. M. 1997, ApJ, 485, 25

Table 1. Direct and derived observables of δ Cephei.

m_V^a	m_I^a	m_K^a	A_V^a	A_I^a	A_K^a	ΔV_r^a	R^a	ΔR^a	μ^a	p^a
4.02	3.23	2.34	0.84	0.53	0.20	47.8	43 ± 2	5.4 ± 0.2	274 ± 11	1.27 ± 0.06

^aApparent V, I, K -band mean magnitudes and luminosity amplitudes (Kiss 1998; Barnes et al. 1997), radial velocity amplitude (km/sec, Bersier et al. 1994), mean radius (solar units, Mérand et al. 2006), radius amplitude (Mérand et al. 2006), true distance (pc, Benedict et al. 2002), p -factor (Mérand et al. 2006).

Table 2. Adopted intrinsic parameters of the best fit models and discrepancies between theory and observations.

Z^a	Y^a	M^a	L^a	T_e^a	R^a	ΔL^a	α^a	p^a	Σ_V^b	Σ_I^b	Σ_K^b	Σ_{Vr}^b	Σ_R^b	σ_V^c	σ_I^c	σ_K^c	σ_{Vr}^c	σ_R^c
0.02	0.28	5.5	3.31	5800	45.06	0.11	0.33	0.94	0.04	0.03	0.01	0.4	0.3	0.9	0.3	0.3	4.2	3.3
0.02	0.26	5.5	3.32	5800	45.07	0.15	0.40	1.15	0.2	0.07	0.008	0.1	0.2	0.2	0.4	0.3	1.6	2.3
0.02	0.24	5.5	3.29	5700	45.32	0.17	0.38	1.03	0.08	0.05	0.01	0.2	0.3	0.1	0.5	0.0	3.0	2.8
0.015	0.27	5.5	3.31	5750	45.29	0.08	0.40	1.18	0.2	0.06	0.009	0.1	0.2	0.5	0.7	0.3	1.6	2.1
0.01	0.26	5.5	3.33	5800	46.07	0.07	0.43	1.28	0.2	0.07	0.01	0.07	0.2	0.6	0.8	0.5	0.4	1.7
0.01	0.24	5.5	3.33	5800	46.08	0.11	0.44	1.21	0.1	0.05	0.009	0.1	0.2	0.5	0.7	0.5	1.0	2.0

^aMetal (Z) and He (Y) abundance by mass, stellar mass (M/M_\odot), logarithmic luminosity ($\log L/L_\odot$), effective temperature (K), radius (R/R_\odot), luminosity excess (dex) respect to canonical ML relation from Bono et al. (2000), convection efficiency parameter (α_{ml}), projection factor required to fit the observed amplitudes.

^bStandard deviations of the fit between the predicted curves and observations over the entire cycle.

^cStandard deviations between observed and predicted amplitudes.

Table 3. Distance and absolute magnitude determinations based on different methods.

Z^a	Y^a	μ_V^a	μ_I^a	μ_K^a	d_1^a	d_2^a	d_3^a	M_V^a	M_I^a	M_K^a
0.02	0.26	7.50	7.37	7.28	271	282	286	-3.51	-4.19	-4.97
0.015	0.27	7.46	7.35	7.29	274	284	288	-3.47	-4.16	-4.97
0.01	0.26	7.52	7.40	7.32	277	288	291	-3.55	-4.23	-5.01
0.01	0.24	7.52	7.40	7.32	277	288	292	-3.54	-4.21	-5.01

^aMetal (Z) and He (Y) abundance by mass; V, I, K apparent distance moduli (mag); true distances (pc) based on the Cardelli et al. (1989) extinction law: $E(B-V) = (\mu_V - \mu_I)/1.22$ (d_1), $E(B-V) = (\mu_V - \mu_K)/2.74$ (d_2); true distances (pc) based on angular diameter variations (d_3); V, I, K absolute magnitudes.)

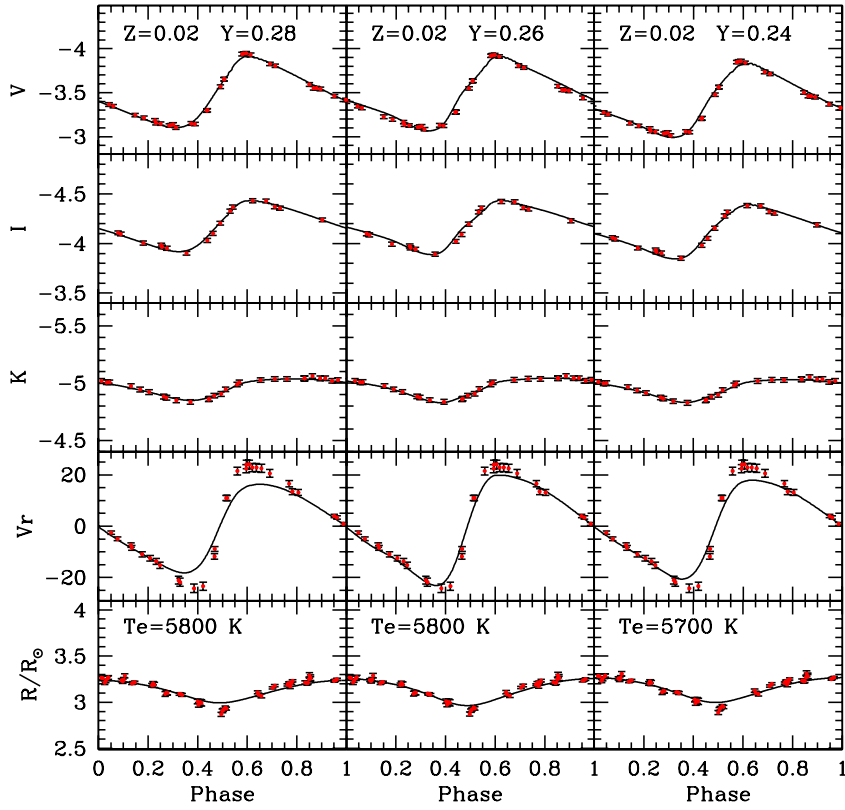


Fig. 1.— Comparison between best fit models at different chemical compositions and observations. From top to bottom V, I, K light curves, radial velocity (km/sec), and radius curve (solar units).

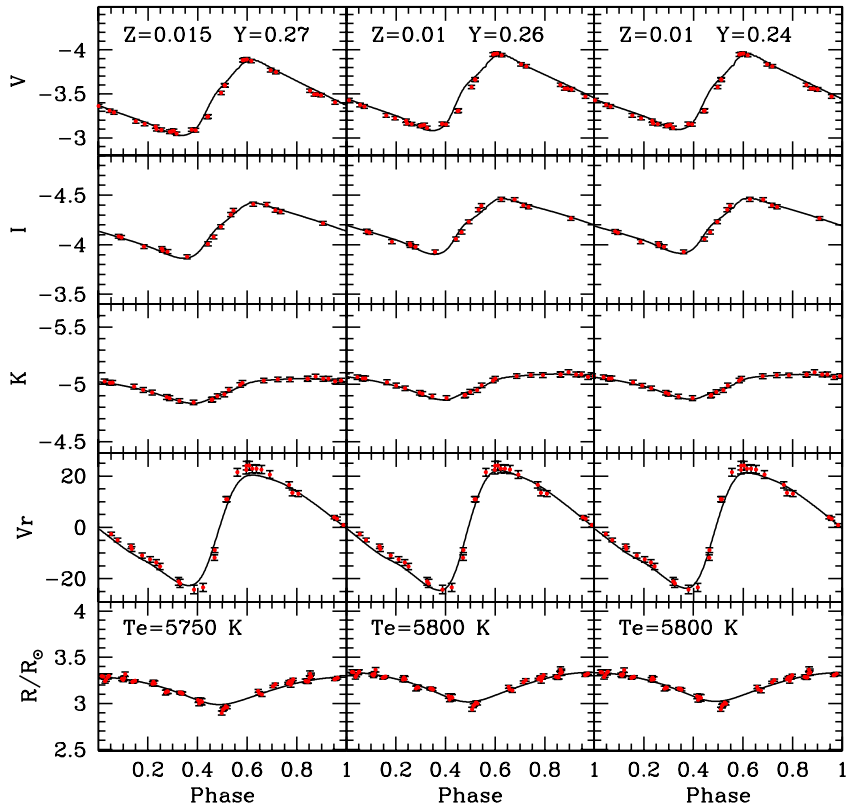


Fig. 2.— Same as Fig. 1, but for more metal-poor best fit models.